Toward an understanding of the single electron data measured at the BNL Relativistic Heavy Ion Collider (RHIC)

P. B. Gossiaux and J. Aichelin
SUBATECH, Université de Nantes, EMN, IN2P3/CNRS, 4 rue Alfred Kastler, F-44307 Nantes cedex 3, France
(Received 6 February 2008; published 17 July 2008)

High transverse momentum (p_T) single nonphotonic electrons which have been measured in the RHIC experiments come dominantly from heavy meson decay. The ratio of their p_T spectra in pp and AA collisions [$R_{AA}(p_T)$] reveals the energy loss of heavy quarks in the environment created by AA collisions. Using a fixed coupling constant and the Debye mass ($m_D \approx gT$) as the infrared regulator, perturbative QCD (pQCD) calculations are not able to reproduce the data, neither the energy loss nor the azimuthal (v_2) distribution. Employing a running coupling constant and replacing the Debye mass by a more realistic hard thermal loop (HTL) calculation, we find a substantial increase in the collisional energy loss, which brings the $v_2(p_T)$ distribution as well as $R_{AA}(p_T)$ to values close to the experimental ones without excluding a contribution from radiative energy loss.

DOI: 10.1103/PhysRevC.78.014904 PACS number(s): 25.75.Dw, 12.38.Mh, 25.75.Gz

I. INTRODUCTION

The spectra of mesons and baryons which contain only light flavors (u, d, s) and which have been produced in ultrarelativistic heavy ion collisions at the BNL Relativistic Heavy Ion Collider (RHIC) accelerator show a remarkable degree of thermalization. Hydrodynamic calculations reproduce quantitatively many of their dynamical properties, and their multiplicity is well described in statistical model calculations. Statistical equilibrium, however, means loss of memory, and therefore hadrons which contain only light flavors are of limited use in the study of the properties of the matter created in the early phase of the reaction.

Heavy quarks, on the contrary, do not come to an equilibrium with the surrounding matter and may therefore play an important role in the search for the properties of this matter. Produced in hard collisions, their initial momentum distribution can be directly inferred from pp collisions. The deviation of the measured heavy meson p_T distribution in AA collisions (divided by N_c, the number of binary initial collisions) from that measured in pp collisions, is usually quantified as $R_{AA} = d\sigma_{AA}/(N_c\, dp_T^2)/(d\sigma_{pp}/dp_T^2)$. R_{AA} is a direct measure of the interaction of the heavy quarks with the environment created in AA collisions. The same is true for the azimuthal distribution, $d\sigma/d\phi \propto [1 + 2v_1 \cos(\phi) + 2v_2 \cos(2\phi)]$, where the v_2 parameter is referred to as "elliptic flow" because at production no azimuthal direction is preferred. The observed finite v_2 value is therefore either due to interactions with light quarks and gluons or due to coalescence at the end of the deconfined phase when the heavy quarks are reshuffled into heavy mesons.

In the RHIC experiments, heavy mesons have not yet been directly measured. Both the STAR [1] and PHENIX [2] Collaborations have observed only single nonphotonic electrons, which have been created in the semileptonic decay of heavy mesons. Thus experimentally one cannot separate between charm and bottom hadrons. pQCD calculations in the fixed order + next to leading logarithm (FONLL) predict a ratio of $\sigma_{\bar{b}b}/\sigma_{\bar{c}c} = 7 \times 10^{-3}$ with the consequence that above $p_T > p_{T\,\mathrm{cross}} \approx 4$ GeV, electrons from bottom mesons dominate the spectrum [3]. The uncertainty of this value is, however, considerable. The little known form of the electron spectrum from heavy meson decay and the little known ratio of heavy quark mesons to heavy quark baryons [4] add to this uncertainty.

To understand the single nonphotonic electron spectra, one has to meet two challenges: one has to understand the interaction of a heavy quark with the environment produced in heavy ion collisions, and one has to understand how this environment changes as a function of time. In the past, several theoretical approaches [5–14] have been advanced to meet these challenges. Almost all of them assume that in the heavy ion reaction a quark-gluon plasma (QGP) is created and that the time evolution of the heavy quark distribution function $f(\vec{p}, t)$ in the QGP can be described by a Fokker-Planck approach:

$$\frac{\partial f(\vec{p},t)}{\partial t} = \frac{\partial}{\partial p_i}\left[A_i(\vec{p}) f(\vec{p},t) + \frac{\partial}{\partial p_j} B_{ij}(\vec{p}) f(\vec{p},t)\right]. \quad (1)$$

In this approach, the interaction of a heavy quark with the QGP is expressed by a drag coefficient [$A_i = \langle (p\text{-}p')_i \rangle$] and by a diffusion coefficient [$B_{ij} = \frac{1}{2}\langle (p\text{-}p')_i (p\text{-}p')_j \rangle$] calculated from the microscopic $2 \to 2$ processes by

$$\langle X \rangle = \frac{1}{2E}\int \frac{d^3k}{(2\pi)^3 2k}\int \frac{d^3k'}{(2\pi)^3 2k'}\int \frac{d^3p'}{(2\pi)^3 2E'} \times n_i(k)(2\pi)^4 \delta^{(4)}(p + k - p' - k')\frac{1}{d_i}\sum |\mathcal{M}_i|^2 X. \quad (2)$$

Here, $p(p')$ and $E = p_0 (E' = p'_0)$ are momentum and energy of the heavy quark (Q) before (after) the collision, and $k(k')$ is that of the colliding light quark (q) or gluon (g) · d_i is 4 for qQ and 2 for gQ collisions. $n(k)$ is the thermal distribution of the light quarks or gluons, which is usually taken as of Boltzmann type. $\mathcal{M}_i$ is the matrix element for the channel i, calculated using pQCD Born matrix elements. Up to now the calculations have been limited to elastic collisions (Qq and Qg). The matrix elements for these channels can be found in Refs. [12,15]. They contain two parameters that have to be fixed: the coupling

constant and the infrared (IR) regulator to render the cross section infrared finite. Up to now, all calculations have used a fixed coupling constant, albeit different numerical values. Usually a Debye mass m_D has been employed as the IR regulator; it is assumed to be proportional to the thermal gluon mass $m_D = \beta g T$, with β around 1.

The Fokker-Planck approaches differ in the way in which the surrounding matter is taken into account. The Texas A&M group [6–8] uses an expanding fireball, whereas the other groups [5,9,10] use hydrodynamic calculations, with different equations of state, however.

Despite the different choices for α_S and m_D and the different models for the expansion of the QGP, all these approaches underpredict by far the modification of the heavy quark distribution due to the QGP. One has to multiply the pQCD cross sections artificially by a K factor of the order of $K \approx 10$ (which depends on the choice of α_S and of the IR regulator) to obtain agreement with experimentally observed values for $R_{AA}(p_T)$ and $v_2(p_T)$ [5,9,10].

One possibility to reduce the value of K has been advanced by van Hees *et al.* [6,7] who assumed that heavy D mesons can be formed in the plasma and decay thereafter isotropically. However, one has to await more precise lattice results to see whether such a nonperturbative process is indeed possible.

It is the purpose of this article to improve these models in three directions. (1) We replace the Fokker-Planck equation by a Boltzmann equation because the momentum transfer is not well parametrized by the first and second moment only. (2) We introduce a physical running coupling constant, fixed by the analysis of e^+e^- annihilation and of the τ decay, in the pQCD matrix elements. (3) We replace the ad hoc parametrization of the infrared regulator by one that yields the same energy loss as the HTL energy loss calculations [16,17]. We will show that with these new ingredients pQCD calculations yield a larger stopping of heavy quarks in matter and bring the results of the calculation close to the experimental values of $R_{AA}(p_T)$ and of $v_2(p_T)$.

We do not address here the radiative energy loss whose importance is highly debated [5,18,19], because detailed microscopic calculations are not yet at hand. They may easily count for the factor of 2 that remains for $R_{AA}(p_T)$ between the data and the calculation which includes collisional energy loss only. This will be the topic of an upcoming publication.

II. INFRARED REGULATOR

To calculate the drag and diffusion coefficients [Eq. (2)] using pQCD Born matrix elements [12,15], the gluon propagator in the t channel has to be IR regulated by a screening mass μ

$$\frac{\alpha}{t} \to \frac{\alpha}{t-\mu^2}. \tag{3}$$

Frequently the IR regulator is taken as the thermal gluon mass [20]

$$\mu^2 = \frac{m_D^2}{3} = \frac{N_c}{9}\left(1+\frac{1}{6}n_f\right)4\pi\alpha_S T^2 \approx \frac{(g_S T)^2}{3}, \tag{4}$$

where $n_f(N_c)$ are the number of flavors (colors) and m_D is the Debye mass. The infrared regulator, however, is not very well determined on first principles. Therefore, in the actual calculations [6–8,12], μ^2 was taken in between $g_S^2 T^2$ and $\frac{g_S^2 T^2}{3}$ with $g_S^2 = 4\pi\alpha_S$. The IR regulator is one of the main sources of uncertainty for the determination of the cross section (and hence for the drag and diffusion coefficients), and it is therefore useful to improve its determination by physical arguments.

For QED, Braaten and Thoma [21] have shown that in a medium with finite temperature, the Born approximation is not appropriate for low momentum transfer $|t|$. It has to be replaced by a hard thermal loop (HTL) approach to the gluon propagator. At high $|t|$ we can use the bare gluon propagator [left-hand side of Eq. (3)]. This approach we call the HTL+hard calculation. To calculate differential cross sections using hard thermal loops is beyond present possibilities, but Braaten and Thoma have shown that in QED the energy loss can be calculated analytically in the HTL+hard approach. Our strategy is now the following: we assume that the gluon propagator can be written in the form

$$\frac{\alpha}{t-\kappa m_D^2(T)}, \tag{5}$$

and we determine the value of κ by requiring that a pQCD Born calculation with this gluon propagator gives the same energy loss as the HTL+hard approach.

We first deal with the QED case where the underlying hypothesis $g^2T^2 \ll T^2$ is more likely to be satisfied and focus our attention on the t channel, which is the only one suffering from IR singularities and therefore decisive for the choice of κ. For the HTL+hard approach, we follow Refs. [21,22] in which the collision of a muon with an electron is calculated. Let us consider the energy loss

$$\begin{aligned}-\frac{dE_\mu}{dx} = \frac{1}{2Ev}\int\frac{d^3k}{(2\pi)^3 2k}\int\frac{d^3k'}{(2\pi)^3 2k'}\int\frac{d^3p'}{(2\pi)^3 2E'}\\ \times n_F(k)(1-n_F(k'))(2\pi)^4\delta^{(4)}(p+k-p'-k')\frac{1}{d}\\ \times\sum|\mathcal{M}_{\mu e\to\mu' e'}|^2\omega,\end{aligned} \tag{6}$$

where v is the velocity of the heavy muon, $\omega = E - E'$ is the energy transfer in the collision, and $d = 4$ is the overall spin degeneracy. The total energy loss is the sum of two contributions:

(i) At small momentum transfer $|t| = |(p\text{-}p')^2| < |t^*|$, where $|t^*|$ is an intermediate scale chosen between $g^2\,T^2$ and T^2, the hard thermal loop regulates the infrared singularity and we obtain [21,22]

$$-\left.\frac{dE_\mu}{dx}\right|_{|t|<|t^*|}^{v\to 1} = \frac{g^4T^2}{48\pi}\ln\frac{6|t^*|}{g^2T^2}. \tag{7}$$

(ii) At large $|t|(|t|_{\max} > |t| > |t^*|)$, no infrared regulator is necessary and we arrive at [21,22]

$$-\left.\frac{dE_\mu}{dx}\right|_{|t|>|t^*|}^{v\to 1} \approx \frac{g^4T^2}{48\pi}\left[\ln\frac{8ET}{|t^*|}-\gamma-\frac{3}{4}-\frac{\zeta'(2)}{\zeta(2)}\right]. \tag{8}$$

Adding the HTL [Eq. (7)] and the hard [Eq. (8)] parts, the intermediate scale t^* disappears, and we arrive at [23]

$$-\left.\frac{dE_\mu}{dx}\right|_{\rm HTL+hard}^{v\to 1} \approx \frac{g^4T^2}{48\pi}\left[\ln\frac{48ET}{g^2T^2}-\gamma-\frac{3}{4}-\frac{\zeta'(2)}{\zeta(2)}\right]. \quad (9)$$

We compare now this result with that obtained by introducing an infrared regulated gluon propagator Eq. (3). In the Born approximation, we obtain the cross section

$$\frac{d\sigma_F}{dt} = \frac{g^4}{\pi(s-M^2)^2}\left[\frac{(s-M^2)^2}{(t-\mu^2)^2}+\frac{s}{t-\mu^2}+\frac{1}{2}\right]. \quad (10)$$

We evaluate here the energy loss for the whole t interval $t \in [t_{\rm min}, 0]$ and obtain (for details, see the Appendix)

$$-\left.\frac{dE_\mu}{dx}\right|_{\rm eff}^{v\to 1} \approx \frac{g^4T^2}{48\pi}\left[\ln\frac{8ET}{e\mu^2}-\gamma-\frac{3}{4}-\frac{\zeta'(2)}{\zeta(2)}\right]. \quad (11)$$

Comparing the pQCD Born [Eq. (11)] with the HTL+hard result [Eq. (9)], we find that μ^2 has to be

$$\mu^2 = \frac{g^2T^2}{6e} = \frac{3}{2e}m_\gamma^2 = \frac{m_D^2}{2e} \Rightarrow \kappa = \frac{1}{2e} \approx 0.2 \quad (12)$$

in order to obtain the same energy loss in QED.

Because QED and QCD have a very similar HTL-propagator structure, the above approach remains valid for QCD as well provided that $\alpha_S \ll 1$ and that μ^2 is replaced by Eq. (4). In the QCD case, however, there is the complication that for temperatures achieved at RHIC, we are at best at the borderline of the range of validity of the HTL approach, $m_D^2 \ll T^2$. As a consequence, the HTL+hard model—commonly used by many authors—is in fact not independent of the intermediate scale t^*. To demonstrate this problem, we start out as in QED. For small $|t|$ we obtain

$$-\left.\frac{dE_Q}{dx}\right|_{|t|<|t^*|} = \frac{C_F\alpha_S}{v^2}\int_{-v}^{v}\frac{x}{(1-x^2)^2} \times \int_{t^*}^{0} dt(-t)[\rho_L+(v^2-x^2)\rho_T], \quad (13)$$

with v being the velocity of the heavy quark Q, and the spectral functions

$$\rho_L(t,x) \equiv -\frac{1}{\pi}\Im\left[\frac{1}{\frac{-t}{1-x^2}+\Pi_L(x)}\right]$$

and

$$\rho_L(t,x) \equiv -\frac{1}{\pi}\Im\left[\frac{1}{t+\Pi_T(x)}\right]. \quad (14)$$

Π_L and Π_T are the self-energies evaluated in the HTL approximation:

$$\Pi_L(x) = m_D^2\left(1-\frac{1}{2}\ln\left|\frac{1+x}{1-x}\right|+\frac{i\pi x}{2}\right),$$
$$\Pi_T(x) = \frac{m_D^2}{2}\left(x^2+\frac{x(1-x^2)}{2}\ln\left|\frac{1+x}{1-x}\right|+\frac{i\pi x(x^2-1)}{2}\right). \quad (15)$$

For large $|t|$ we obtain [see Eq. (6)]

$$-\left.\frac{dE_Q}{dx}\right|_{|t|>|t^*|} = \sum_i \frac{1}{2Ev}\int\frac{d^3k}{(2\pi)^3 2k}\int\frac{d^3k'}{(2\pi)^3 2k'} \times \int\frac{d^3p'}{(2\pi)^3 2E'}\Theta(|t|-|t^*|) \times n_i(k)(1\mp n_i(k')) \times (2\pi)^4\delta^{(4)}(p+k-p'-k') \times \frac{1}{d_i}\sum|\mathcal{M}_i|^2\,\omega. \quad (16)$$

Here the matrix elements include $qQ \to qQ$ as well as $gQ \to gQ$ collisions. In contradistinction to the QED case, the sum of both terms depends explicitly on the intermediate scale t^* in the region $[m_D^2, T^2]$, as seen in Fig. 1.

There we display the two parts of the energy loss [Eq. (13) blue dotted, and Eq. (16) purple dashed) as well as the sum of both (purple full). Clearly, the total energy loss becomes stationary with respect to the intermediate scale $|t^*|$ only for a value of $|t^*| \approx 0.4$ GeV$^2 \gg T^2(= 0.0625$ GeV$^2)$

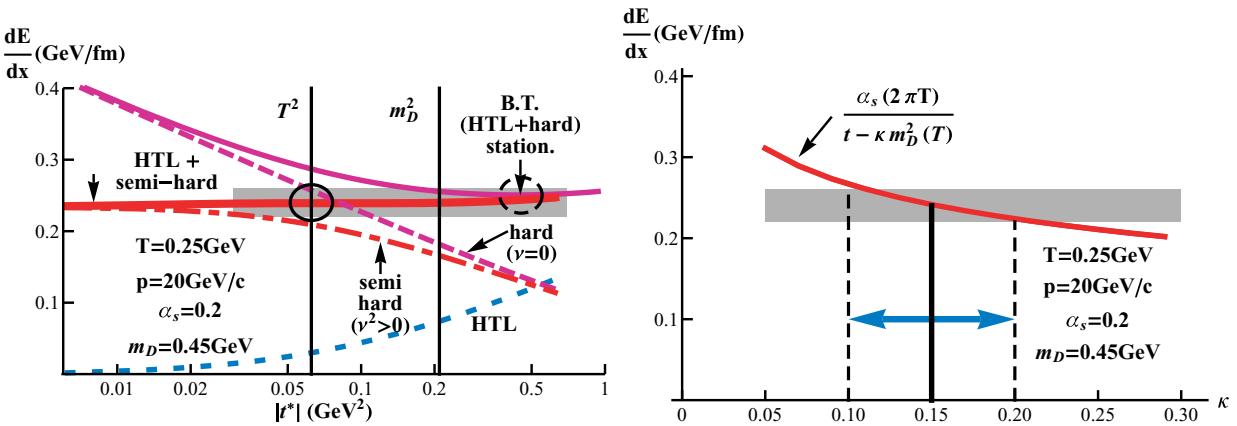

FIG. 1. (Color online) Left: Total energy loss in the HTL+hard approach as well as the different components for a given choice of parameters as a function of the intermediate scale t^*. The full lines are the sum of the HTL (blue dotted) and hard/semihard parts (dashed purple for $\nu^2 = 0$, dashed-dotted red for $\nu^2 \approx 0.16m_D^2$). Right: Total energy loss evaluated with Born cross sections and with the propagator, Eq. (5), as a function of κ. Only the t-channel contribution has been considered here.

and hence in a region where the HTL approach is not valid anymore. Mathematically, this is due to the appearance of terms $\propto O(m_D^2/|t^*|)$ and $\propto O(|t^*|/T^2)$ which are not small nor do they compensate. Physically, we are in a regime where the interaction is screened over a distance of the same order as the mean distance between QGP constituents, so that a large part of the "hard collisions" will be affected by the medium polarization as well. Our prescription to cure this problem is to add an IR regulator ν^2 to the hard part [as μ^2 in Eq. (3)]. We dubbed this approach therefore "semihard." The HTL part remains unchanged. The value of ν^2 is chosen in such a way that for a wide range of temperatures and heavy-quark momenta, the sum of the HTL and semihard energy loss is independent of $t^\star$ for $|t^\star| < T^2$, i.e., in the range where the HTL approximation holds. The red bold line in Fig. 1 shows this independence of the total energy loss on $t^\star$ when the hard part is replaced by the semihard (red dashed dotted) approach for $p = 20$ GeV, $T = 0.25$ GeV, and $\nu^2 \approx 0.16 m_D^2$. We will adopt this value of ν^2 for the subsequent calculations.

If we compare the t-channel energy loss calculated in the HTL+semihard approach (shaded area in Fig. 1) with that obtained within our pQCD Born approach [Eq. (5)] we find a value of κ around 0.15. This value is close to that obtained in QED [Eq.(12)]. It is considerably lower than those used up to now in the pQCD cross section calculation. This is our first seminal result.

III. RUNNING COUPLING CONSTANT

The constant coupling constant α_S is the other quantity that limits the predictive power of the present calculations. In the published calculations, α_S was taken in between 0.2 [21] and 0.6 [12], leading to a difference of a factor of 9 for the drag and diffusion coefficients.

As has been observed by Dokshitzer [24], there exists the possibility to define a running coupling that stays finite in the infrared by writing observables as a product of a universal effective time-like coupling and a process-dependent integral. An alternative approach is to define an effective coupling constant $\alpha_{\rm eff}(Q^2)$ from the analysis of physical observables. Two different experiments, e^+e^- annihilation [25] as well as nonstrange hadronic decays of τ leptons [26], have been used to determine the infrared behavior of $\alpha_{\rm eff}(Q^2)$. The resulting coupling constants are infrared finite and very similar. These effective couplings are all-order resummations of perturbation theory and include all nonperturbative effects. We extend the parametrization of the time-like sector [24] to the space-like sector, which leads to

$$\alpha \to \alpha_{\rm eff}(Q^2) = \frac{4\pi}{\beta_0} \begin{cases} L_-^{-1} \\ \frac{1}{2} - \pi^{-1}\mathrm{atn}(L_+/\pi) \end{cases} \quad \text{for} \quad Q^2 \leqslant 0, \tag{17}$$

with $\beta_0 = 11 - \frac{2}{3}n_f$, $n_f = 3$, and $L_\pm = \ln(\pm Q^2/\Lambda^2)$. In the space-like sector, we replace the propagator

$$\frac{\alpha}{t} \to \frac{\alpha_{\rm eff}(t)}{t - \mu^2}, \tag{18}$$

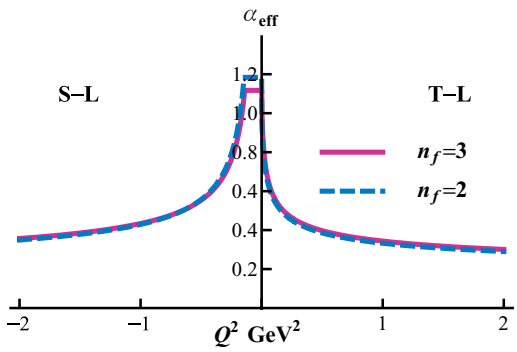

FIG. 2. (Color online) Q^2 dependence of the running coupling constant.

where μ^2 is an IR regulator which we will specify below. The coupling constant $\alpha_{\rm eff}$ is displayed in Fig. 2 for two and three flavors.

It has already been argued in Ref. [27] that a running coupling constant leads to the disappearance of the logarithmic E dependence of the energy loss at large energies, that is,

$$\frac{dE}{dx} \propto \alpha_S(2\pi T)^2 T^2 \ln\frac{ET}{m_D^2} \longrightarrow \frac{dE}{dx} \propto \alpha_S(\mu^2) T^2, \tag{19}$$

with an IR regulator $\mu^2 = \left[\frac{1}{2}, 2\right]\tilde{m}_D^2$, where the Debye mass $\tilde{m}_D$ is determined self-consistently according to

$$\tilde{m}_D^2(T) = \frac{N_c}{3}\left(1 + \frac{1}{6}n_f\right) 4\pi\, \alpha(-\tilde{m}_D^2(T))\, T^2. \tag{20}$$

However, this ambiguity of the coefficient leads to a nonnegligible uncertainty in the energy loss.

In this work, we determine the optimal infrared regulator using the same strategy as for the nonrunning case: we calibrate the energy loss to the one obtained in a generalized "HTL+semihard" approach this time with a running coupling constant. For this purpose, we assume that the (squared) Debye mass for a fixed coupling constant appearing in the hard thermal loop terms [Eq. (15)], $m_D^2(T) \equiv (1 + \frac{n_f}{6})g^2T^2$, can be replaced by $m_D^2(T,t) \equiv (1 + \frac{n_f}{6})4\pi\alpha_{\rm eff}(t)T^2$. As illustrated in Fig. 3 (left, full purple line), here also the total energy loss depends on the intermediate scale $|t^\star|$ in the domain of validity of the HTL approach, if we employ the HTL+hard approach. Only if we replace the hard by a semihard propagator, that is,

$$\frac{\alpha_{\rm eff}(t)}{t} \longrightarrow \frac{\alpha_{\rm eff}(t)}{t - \lambda m_D^2(T,t)}, \tag{21}$$

may we obtain an energy loss that is independent of the intermediate scale $t^\star$. The optimal choice is $\lambda \approx 0.11$ (see Fig. 3, left, bold red line).

Using this prescription, the energy loss in the t channel is found to be ≈1.3–1.4 GeV/fm, i.e., ≈6 times larger than the energy loss found with the same parameters for the nonrunning coupling constant. For $|t^\star| < T^2$, the HTL contribution becomes negligible, and the energy loss is given by the semihard part only (which is IR-convergent). Therefore, the natural IR regulator μ^2 for our effective Born pQCD approach [Eq. (18)] is $\mu^2 = \kappa m_D^2(T,t)$, with $\kappa \approx \lambda \approx 0.11$, i.e., exactly the propagator of the right-hand side of Eq. (21).

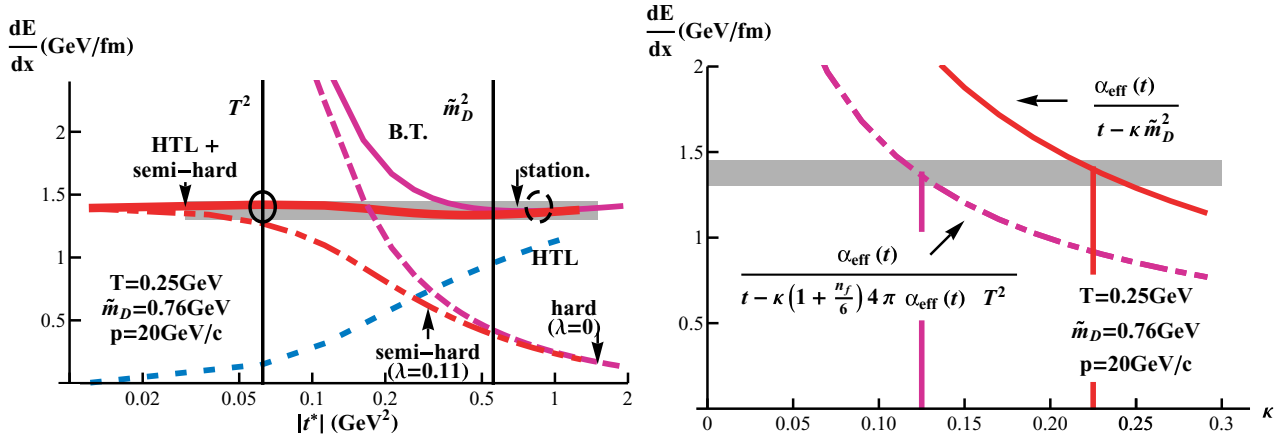

FIG. 3. (Color online) Left: Same quantities as in Fig. 1, but for the case of a running $\alpha_{\rm eff}$. Right: Total energy loss in the pQCD Born approximation for two different IR regulators as a function of κ. The shaded area corresponds to the energy loss calculated in the HTL+semihard approach (left).

However, the same energy loss can be obtained if one uses the simpler propagator of Eq. (18) taking $\mu^2 = \kappa \tilde{m}_D^2(T)$, that is,

$$\frac{\alpha_{\rm eff}(t)}{t - \kappa \tilde{m}_D^2(T)}, \tag{22}$$

with $\kappa \approx 0.2$ and $\tilde{m}_D$ the Debye mass defined self-consistently according to Eq. (20). This is shown on the right-hand side of Fig. 3 and leads to our choice $\mu^2_{\rm QCD} = 0.2\,\tilde{m}_D^2(T)$ for the propagator defined by Eq. (18). We will show later that with these values, the drag coefficient and hence the energy loss differs only slightly between these two models in the (T, p) range of interest for ultrarelativistic heavy ion collisions. We note in passing that a similar energy loss has been obtained by Wick *et al.* [28] in a simpler model for light quarks.

IV. RESULTS

To evaluate the consequences of our new approach, we compare the results with those obtained for other choices of coupling constants and infrared regulators. They are summarized in Table I. From A → F the parametrizations become increasingly realistic.

For the results presented below, we include the s and u channels as well. They do not require any IR regulator, and the coupling constants have been chosen as $\alpha \to \alpha_{\rm eff}(s - m^2)$ and $\alpha \to \alpha_{\rm eff}(u - m^2)$ because $s = m^2$ and $u = m^2$ correspond to the maximal "softness" in these channels.

A. Cross sections

The cross sections $\frac{d\sigma}{dt}$ for the different parametrizations of Table I are displayed in Fig. 4, left for quarks and right for gluons. It is evident that both a running coupling constant and a lower IR regulator increase the cross section at small t, whereas the increase at high t is rather moderate but nevertheless visible in the gQ reactions due to the u channel.

B. Individual collisions and transport coefficients

For many interpretations, it is interesting to see how the quarks lose their energy when traversing a plasma of a given temperature. For this purpose, we study the differential probability $P_i(w, p)$ that a heavy quark with a momentum p in the rest system of the heat bath loses the energy w by colliding with a plasma particle of type i:

$$P_i(w, p) \equiv \int \frac{d^3k}{(2\pi)^3} \frac{n_i(k)}{2k} \int_{t_-}^{t_+} \frac{dt}{\sqrt{H}} \sum |\mathcal{M}_i|^2. \tag{23}$$

TABLE I. Coupling constants and IR regulators used in our calculations and their graphic representations in the figures.

	α_S	μ^2	Line form	Line color
A	0.3	m_D^2	Dotted thin	Black
B	$\alpha_S(2\pi T)$	m_D^2	Dashed thin	Black
C	$\alpha_S(2\pi T)$	$0.15 m_D^2$	Full thin	Black
D	Running, Eq. (17)	$\tilde{m}_D^2$	Dashed bold	Red
E	Running, Eq. (17)	$0.2\tilde{m}_D^2$	Full bold	Red
F	Running, Eq. (17)	$0.11(6\pi\,\alpha_{\rm eff}(t)\,T^2)$	Dashed dotted bold	Purple

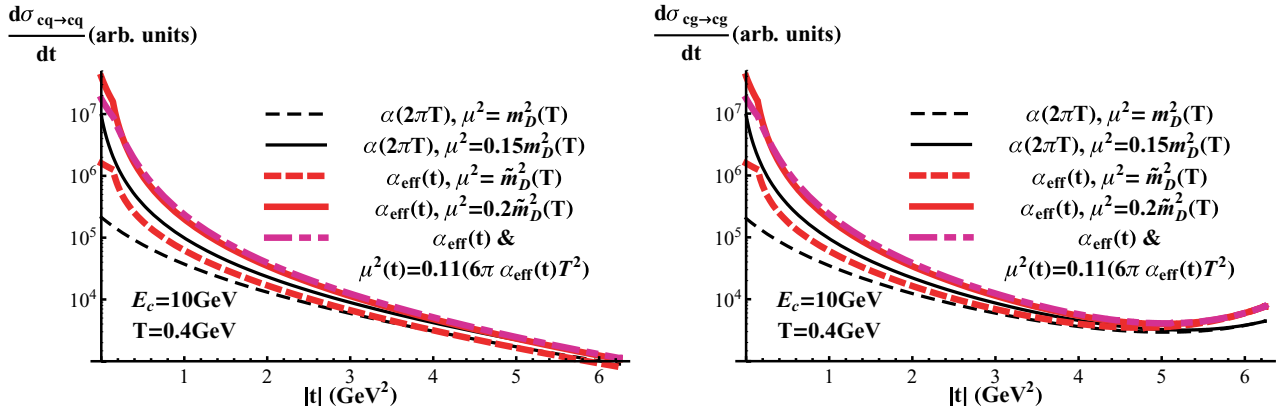

FIG. 4. (Color online) Effective cross section $d\sigma/dt$ for the different models (see Table I).

The condition $H \geqslant 0$, where

$$H = (4\pi)^4 E^2 \{[s-(E+k)^2]t^2 + [(2Ek - s + m_c^2)^2 - 4k^2p^2 + 2w[k(s+m_c^2) - E(s-m_c^2)]]t - w^2(s-m_c^2)^2\}, \quad (24)$$

with $s = m_c^2 + 2Ek(1-\cos\theta(\vec{k},\vec{p}))$, determines not only the limits $t_\pm$ in Eq. (23), it also constrains the integral over $\vec{k}$.

The probability $P_i(w, p)$ for a charm quark (c-quark) with $p = 10$ GeV in a plasma with temperature $T = 400$ MeV is displayed in Fig. 5. On the left (right) side we see the probability for cq (charm quark-quark collisions) collisions. Negative values of w mean that the heavy quark gains energy in the collision. Due to the u-channel contribution, cg collisions are more effective in transferring a large amount of energy. The large majority of the collisions yield only a small energy transfer. To show which collisions are most important for the total energy loss of the c-quark, we display in Fig. 6 (left) (the absolute value of) $w\,P_q(w, p)$ for cq collisions. (Cq collisions would exhibit a similar behavior). This quantity is directly related to the differential energy loss:

$$\frac{dE_q}{dx\,dw} = v^{-1} P_q(w, p)\, w. \quad (25)$$

Collisions with a small energy transfer become dominant when a running coupling constant is employed. Figure 6, right, shows

$$\int^{w} dw' \frac{dE_q}{dx\,dw'} \Big/ \int^{\infty} dw' \frac{dE_q}{dx\,dw'} \quad (26)$$

and displays that collisions with an energy transfer of $w < 1$ GeV contribute 70% of the total energy transfer in our new approach, whereas in the standard model (B) they contribute only 25%.

To make our calculation comparable with other Fokker-Planck calculations, we present in Fig. 7 the drag coefficient A as a function of the heavy-quark momentum p [left for charm quarks (c-quarks) and right for bottom quarks (b-quarks)]. The calculations for the two fixed coupling constants $\alpha_S = 0.3$ and $\alpha_S(2\pi\,T)$ do not yield different drag coefficients as long as the IR regulator is the same. Therefore we do not pursue model A. If one changes the IR regulator from the standard value, m_D^2, to that reproducing the HTL energy loss ($\kappa = 0.15$), one observes an increase by a factor of 2. A running $\alpha_S(\alpha_{\rm eff})$ with a standard IR regulator increases the drag coefficient for low momenta where the small-t exchanges are more important. If the low-t collisions are enhanced by both a running α_S and a small IR regulator, we see an increase of the drag coefficient by a factor of $\approx$5. The drag does not change substantially if the IR regulator is calculated with a running coupling constant—

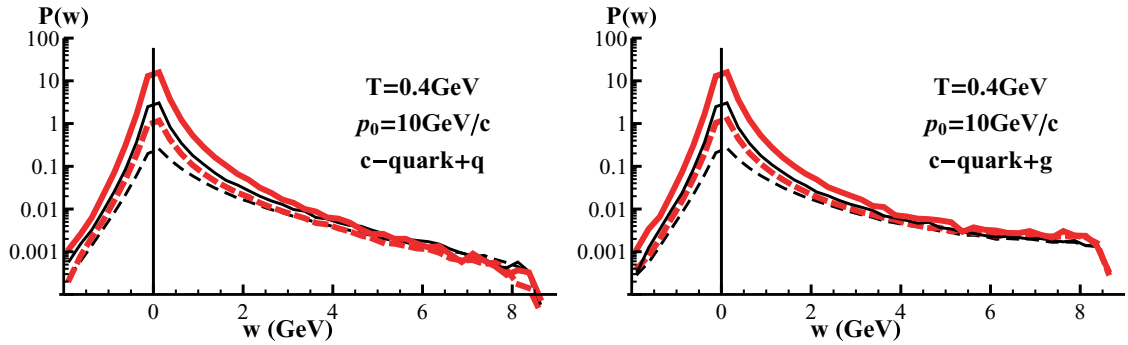

FIG. 5. (Color online) Differential probability $P(w)$ that a c-quark with an initial momentum of $p = 10$ GeV/c loses the energy w in a collision with a plasma particle in a plasma at $T = 400$ MeV, for collisions with quarks (left) and for collisions with gluons (right). For the different curves, see Table I.

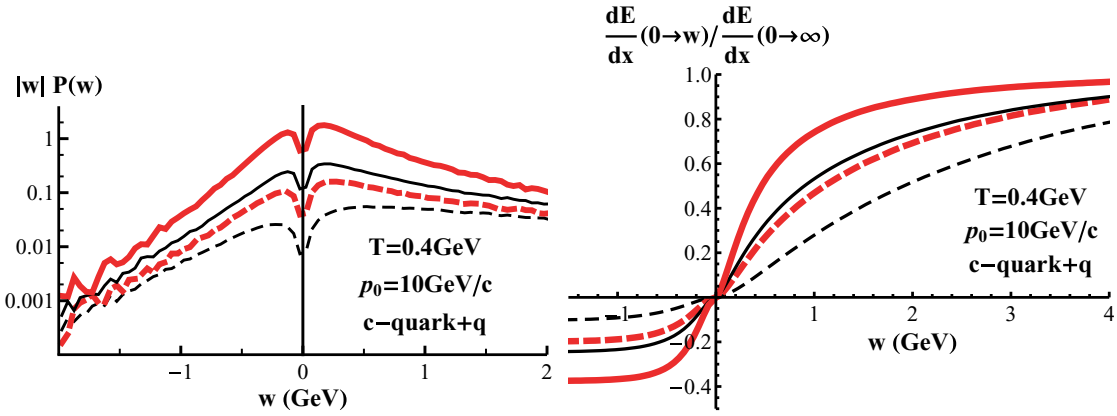

FIG. 6. (Color online) Differential energy loss $w\,P_q(w) = \frac{dE_q}{dt\,dw}$ (left) and its normalized integral (right), both evaluated for a heavy quark with an initial momentum of $p = 10$ GeV/c colliding with a quark. For the different curves, see Table I.

model F—as compared with model E, and we therefore discard model F from further calculations. If α_S remains fixed, the drag coefficient remains moderate for all IR regulators, as it does for a running α_S and the Debye mass as IR regulator. Bottom quarks show a similar behavior but because of their higher mass, their drag coefficient is around 30–40% smaller than that of the c-quarks. For a given plasma-lifetime evolution, we thus expect a smaller energy loss of b-quarks, but it is far from being negligible, especially in the most realistic models E and F.

The drag coefficient depends strongly on the temperature. In Fig. 8, we display that of a c-quark with a momentum of 10 GeV/c. As expected in our model, a hot plasma is much more effective for quenching a fast quark than a cold plasma.

C. Nucleus-nucleus collisions

Having discussed single Qq and Qg collisions, we investigate now the consequences of our approach for heavy quark observables in ultrarelativistic heavy ion collisions. To study the time evolution of the heavy quark in a plasma, usually a Fokker-Planck equation has been used. This approach has several shortcomings. (a) The drag and diffusion coefficients, calculated by Eq. (2), do fulfill the Einstein relation only in leading logarithmic order E/T [5]. This is not sufficient to ensure the thermalization of the heavy quark [29]. Either one has to impose the Einstein relation, or the asymptotic heavy quark distribution is a Tsallis function and not a Boltzmann distribution. (b) Being a small scattering angle approximation (or, in other words, containing the leading order term of T/E_Q only), the approach brakes down if the momenta of the qg and of the Q are of the same order, i.e., in the region where v_2 becomes large. (c) Even for large energies E_Q, the first and second moments only [Eq. (2)] are not a good approximation of the energy loss. It can be seen in Fig. 4 (right) that hard transfers are not excluded in the gluonic channel because of the QCD equivalent of the Compton effect.

Therefore, for the calculation presented here, we use a Boltzmann equation approach as in Ref. [11] in a test particle version. In coordinate space, the initial distribution of the heavy quarks is given by a Glauber calculation. For the momentum space distribution as well as for the relative contribution of charmed and bottom quarks, we use the pQCD results of Ref. [3]. In the E866 experiment at Fermi Lab [30], it has been observed that in pA collisions, J/ψ mesons have a larger transverse momentum than in pp collisions. This effect,

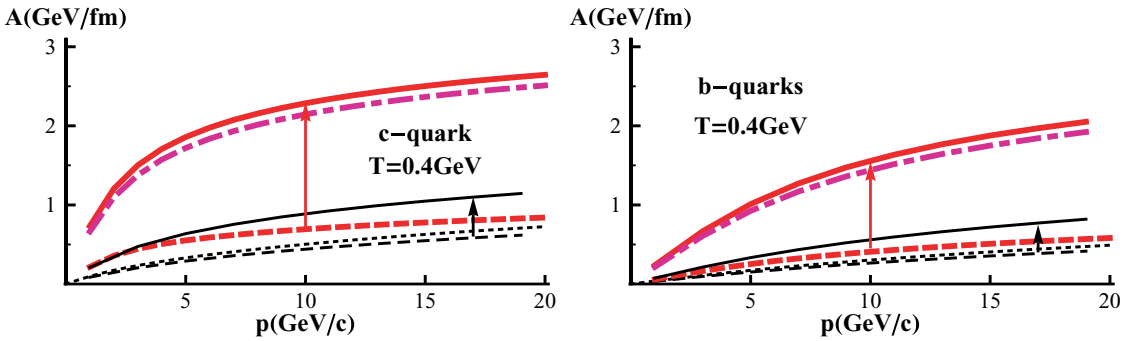

FIG. 7. (Color online) Drag coefficient A (left for charm quarks, right for bottom quarks) as a function of the heavy quark momentum p. We display A for temperature $T = 400$ MeV and for different combinations of coupling constants and IR regulators as defined in Table I. For the different curves see Table I.

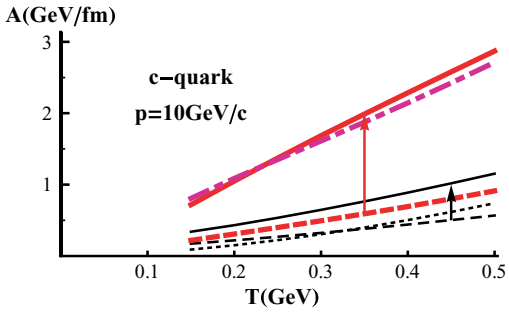

FIG. 8. (Color online) Temperature dependence of the drag coefficient A for c-quark with momentum $p = 10$ GeV/c. For the different curves see Table I. The arrows show how the drag coefficients change if one replaces m_D by the IR regulator determined by the HTL+semihard approach.

called the Cronin effect, can be parametrized as an increase of $\langle p_T^2 \rangle$ by $\delta_0 \approx (0.2\ \text{GeV})^2$ per collision of the incident nucleon with one of the target nucleons. For most of the calculations, we then convolute the initial transverse-momentum distribution of the heavy quark [3] with a Gaussian of rms $\sqrt{n_{\text{coll}}(\vec{r}_\perp)\,\delta_0}$. In this parametrization, n_{coll} is taken as the mean number of soft collisions which the incoming nucleons have suffered prior to the formation of the $Q\bar{Q}$ pair at transverse position $\vec{r}_\perp$. Future studies of D-meson/B-meson production at RHIC may allow one to improve this choice.

In our approach, we then follow the trajectories of the individual heavy quarks in the expanding plasma, described by the hydrodynamic model of Kolb and Heinz [10,31]. We parametrize the temperature $T(r,t)$ and the velocity $u_\mu(r,t)$ field of this model and use this parametrization in a finite time step method to calculate the collision rate Γ [Eq. (2) with $X = 1$] for $Qg \to Qg$ and $Qq \to Qq$ reactions [12,15] and for the different parametrizations of the cross section. For a given interval of the (Bjorken) time $\Delta\tau$, we then generate the number of collisions according to a Poisson distribution of average $\Gamma\Delta\tau$ and perform these collisions individually. When a collision takes place, we determine the final momentum of the heavy quark by taking randomly a scattering angle with a distribution given by the cross section at a given temperature. In this method, no small angle approximations are necessary, and we arrive by definition at a thermal distribution if we place the heavy quark in infinite matter at a given temperature.

As the time-point of the hadronization of the plasma is not well determined, we explore here two options: hadronization of heavy quarks into D(B) mesons when the expanding system enters the mixed phase and at the end of the mixed phase. In the latter option, more collisions are possible, and we expect therefore a larger quenching of heavy quarks. Also for the hadronization, we apply two approaches that give slightly different meson momentum distributions: (1) we apply exclusively the fragmentation mechanism as in p-p [3] or (2) we apply the fragmentation mechanism for high momentum quarks only; whereas at low momentum, heavy mesons are formed by coalescence. For this purpose, we define the probability distribution g that a heavy meson of momentum $\vec{P}$ is formed by coalescence of a heavy quark with momentum $\vec{p}_Q$ with a light quark as

$$g(\vec{P}, \vec{p}_Q) = \beta \int d^3q\, n(q,T)\, f(\vec{q} - \vec{p}_Q)\, \delta(\vec{P} - \vec{p}_Q - \vec{q}), \quad (27)$$

where $n(q,T)$ is the thermal momentum distribution of the light quarks at the moment of hadronization and f is the probability density that the heavy quark with momentum $\vec{p}_Q$ forms a heavy meson with a light quark of momentum $\vec{q}$. In the calculation, we evaluate g in the fluid rest frame and take f as a boosted Gaussian. β is chosen such that g is normalized to unity for $\vec{p}_Q = 0$. Finally, the heavy meson undergoes a weak decay and creates the single electrons observed in the detector.

The results for R_{AA} in central Au+Au collisions are compared with the experimental data in Fig. 9. From top to bottom we show the results for the approaches B–E of Table I. On the left, we present the results for a hadronization at the beginning of the mixed phase; on the right, for a hadronization at the end of the mixed phase. We observe that the additional interactions in the mixed phase reduce the artificial K factor, shown in the figure, with which the pQCD cross section has to be multiplied to describe the data. For some of the curves, we present the results for two different values of K; in others, we show the influence of the different approaches for fragmentation. The label "fragm." means that heavy mesons are exclusively created by fragmentation; "coal.+fragm." means that they are rather produced by coalescence at low momentum. It is evident that the different hadronization scenarios have little influence on the K factor, which is necessary to describe the data. For a constant coupling constant and the Debye mass as the IR regulator (model B), one has to employ K factors of the order of 10–12. A smaller IR regulator (model C) or a running coupling constant (model D) reduces this K factor to values of 5–10, still much too large to render the calculation understandable. Only the combination of both (model E) brings the K factor close to an acceptable value of 1–2, leaving nevertheless still room for radiative energy loss.

A very similar observation can be made for the minimum bias calculations, which are compared with the experimental data in Fig. 10. On the left, we display the results for model B; on the right, for model E. For a fixed coupling constant and the Debye mass as the IR regulator we need, as for central collisions, a K factor of around 12; whereas for model E, the K factor is reduced to 1.5–2. Thus for central and minimum bias calculations, the same K factors have to be employed, a minimal requirement for the validity of this reaction scenario.

The Cronin effect changes the R_{AA} value only for momenta between 1 and 3 GeV, as can be seen in Fig. 11. It is therefore without any importance for the understanding of the R_{AA} values at large p_T but brings R_{AA} much closer to the data in the p_T range where the v_2 values are large.

We come now to the discussion of v_2. To our knowledge, the present theories based on pQCD have not succeeded to describe *simultaneously* the experimental R_{AA} and v_2 results. As shown in Fig. 12, left, for model B neither the Cronin effect nor an augmentation of the K factor beyond the value needed to describe R_{AA} increases v_2 considerably. What helps is a larger interaction time, i.e., a late freeze-out. This is shown in Fig. 12, right, where we compare the v_2 values for a hadronization at the beginning and at the end of the mixed phase. Using a fixed

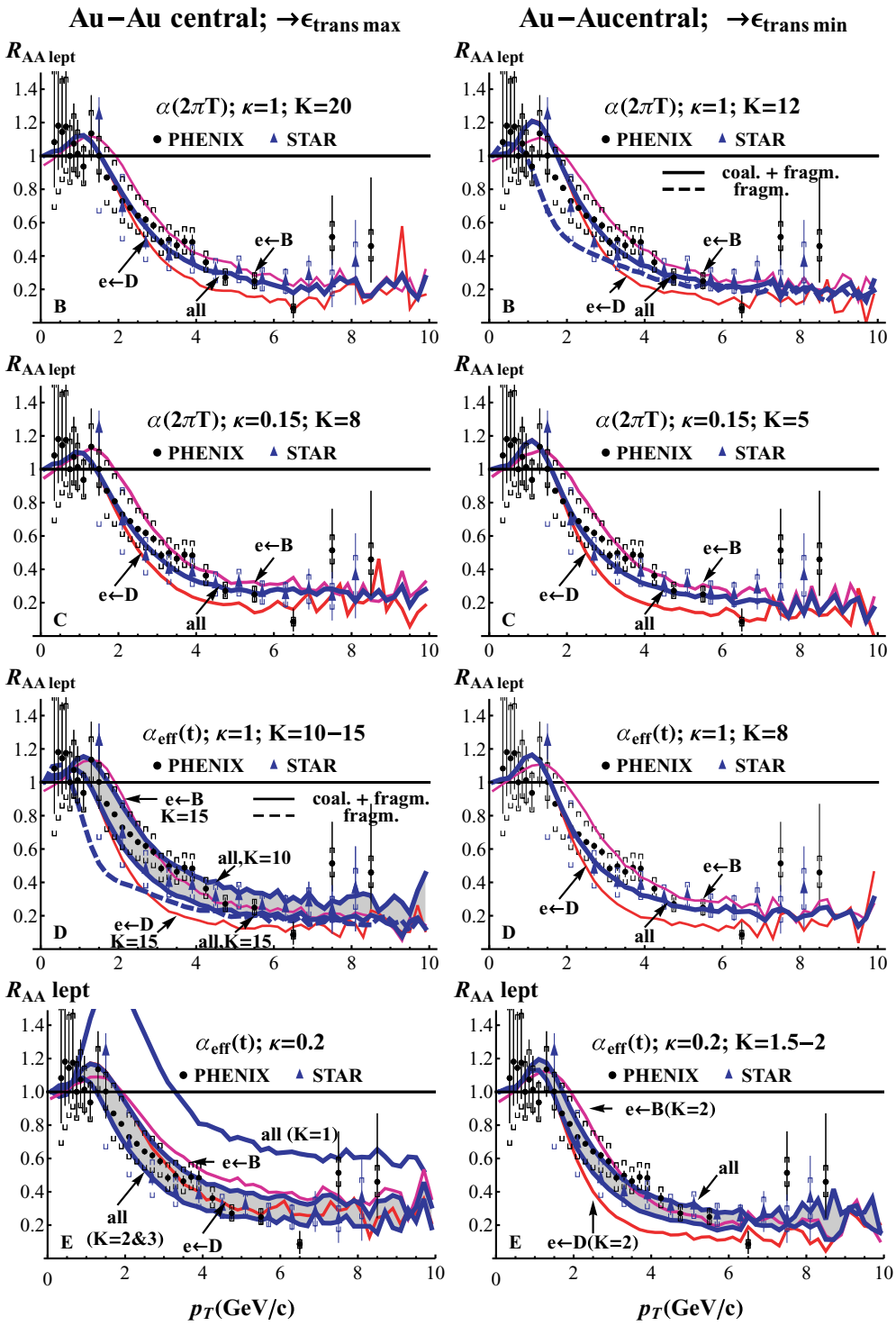

FIG. 9. (Color online) Comparison of experimental and theoretical results for central Au+Au collisions. We display R_{AA} of single nonphotonic e^- as a function of the heavy quark momentum p_T. The purple line shows R_{AA} for e^- from B-meson; the red line that of D-meson decay for the K values indicated. The blue line is the sum of both. On the left, we assumed hadronization at the beginning of the mixed phase; on the right, at the end of the mixed phase. From top to bottom, we display the results for the parametrizations B–E (see Table I).

coupling constant, the K factors remain large, however. If one combines a running α_S with a HTL+semihard IR regulator, one can reproduce $v_2(p_T)$ using a K factor slightly larger than 2 and assuming a late freeze-out as can be seen in Fig. 13.

One could imagine that azimuthal correlations of nonphotonic e^+-e^- pairs created in the decay of the heavy mesons whose heavy quarks have been created together may carry information on the energy loss mechanism. Many

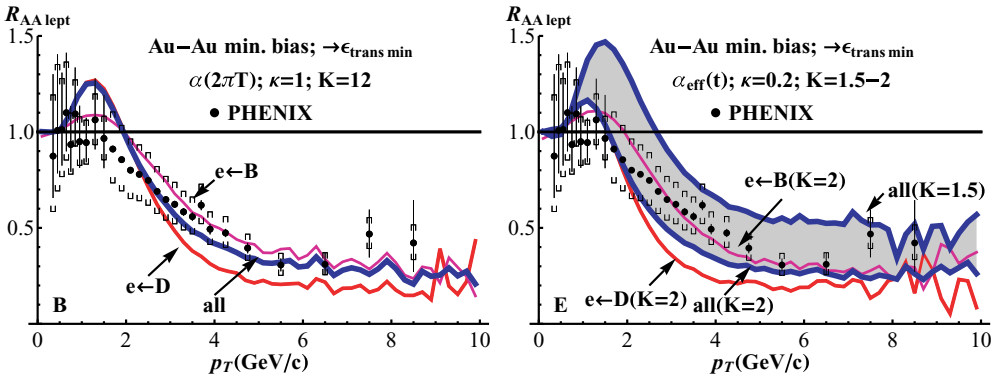

FIG. 10. (Color online) Comparison of experimental and theoretical results for minimum bias Au+Au collisions, using model B (left) and model E (right). We display R_{AA} of single nonphotonic e^- as a function of the heavy quark momentum p_T. The red line shows the e^- for D-meson decay, the purple line those for B-meson decay, and the blue thick line the sum of both. Hadronization is assumed to take place at the end of the mixed phase. The applied K factors are given; the Cronin effect is taken into account.

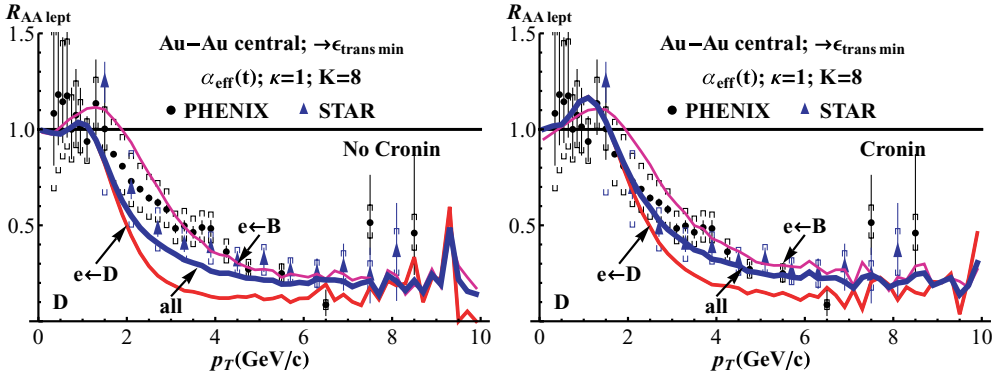

FIG. 11. (Color online) Influence of the Cronin effect on the R_{AA} of single nonphotonic e^- as a function of the heavy quark momentum p_T. The red line shows the e^- from D-meson decay, the purple line those from B-meson decay, and the blue thick line the sum of both. We assumed hadronization at the end of the mixed phase. We display the results without (left) and with (right) the Cronin effect, both for model E (see Table I).

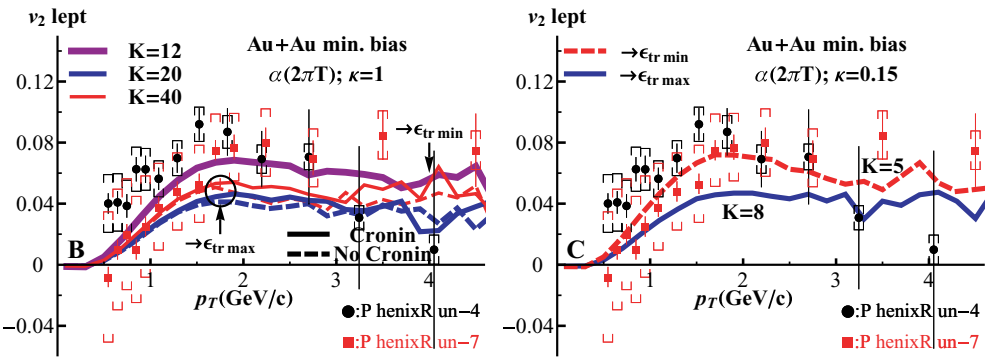

FIG. 12. (Color online) Dependence of the v_2 of single nonphotonic e^- as a function of the heavy quark momentum p_T on the Cronin effect and on the K factor (left) as well as on the freeze-out density and IR regulator (right). All calculations are done with $\alpha_S(2\pi T)$.

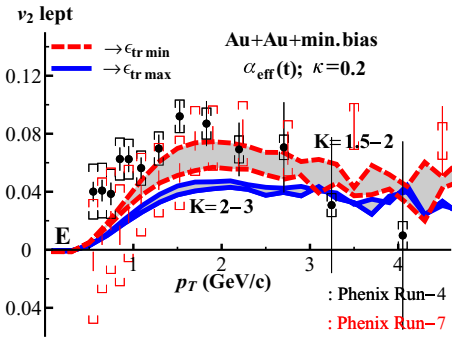

FIG. 13. (Color online) v_2 of single nonphotonic e^- as a function of the heavy quark momentum p_T for different freeze-out energies using a running coupling constant and a small IR regulator (model E).

collisions with small momentum transfer may better conserve the original back-to-back correlations than few collisions with a large energy transfer. As displayed in Fig. 14, this is not the case. Models A and E give about the same azimuthal correlation. This means, on the other hand, that correlations are a quite robust observable for testing this reaction scenario and confronting it with other ideas such as the anti-de-Sitter space/conformal field theory (AdS/CFT) approach [32].

V. CONCLUSION AND OUTLOOK

In conclusion, we have found that it is possible to reduce the uncertainties inherent in present-day calculations of the energy loss and $v_2(p_T)$ distribution of heavy quarks traversing a quark gluon plasma by (a) determining the infrared regulator by the requirement that it reproduces the energy loss calculated in the hard thermal loop + semihard approach and (b) using an effective infrared-safe physical coupling constant that describes other data such as gluon radiation in e^+e^- annihilation and the nonstrange decay of τ leptons.

Results of calculations in which these new features are employed come close to the experimental data for $R_{AA}(p_T)$ as well as for $v_2(p_T)$. The K factor required to reproduce the data is between 1.5 and 2. Up to now, a simultaneous description of R_{AA} and v_2 has not been possible even with large K factors. That the K factor is above unity may be due to radiative processes which are not included here, but it may also be due to the lack of a detailed knowledge of the different physical processes involved. They include the initial distribution of charm and bottom quarks, their hadronization, and the role of heavy baryons.

This observation has importance far beyond the physics of heavy mesons. Because the same running coupling constant and the same infrared regulator appear also in the cross section for light quarks, we expect a similar energy loss for light quarks. Pions show indeed a very similar $R_{AA}(p_T)$ distribution, but baryons do not. The reason for this is unknown, but if one follows the idea that they are formed by coalescence, their formation mechanism may be rather different from that of heavy mesons. This conjecture is supported by their large v_2 values. In addition, the large collective radial flow counteracts the individual energy loss. To clarify the hadronization mechanism of light hadrons, one probably has to wait until jet-like hadrons and those created by the plasma hadronization can be separated, either by measuring correlations or by extending the detection range in momentum space in future CERN Large Hadron Collider (LHC) experiments.

The observed enhanced cross section may also be of importance for the understanding of the fast equilibration observed in the entrance channel of ultrarelativistic heavy ion collisions where we do not have a heat bath like here but rather a momentum distribution given by the structure functions. There, however, the typical momentum is not far from that of the heat bath particles.

ACKNOWLEDGMENTS

We thank A. Peshier and S. Peigné for fruitful discussions and R. Vogt for her communication on details of the approach of Ref. [3].

APPENDIX

A. HTL+hard

As the large transfer t will bring the parton to a final state k' for which $n_F(k') \ll 1$, we neglect the factor $1 - n_F(k')$ for

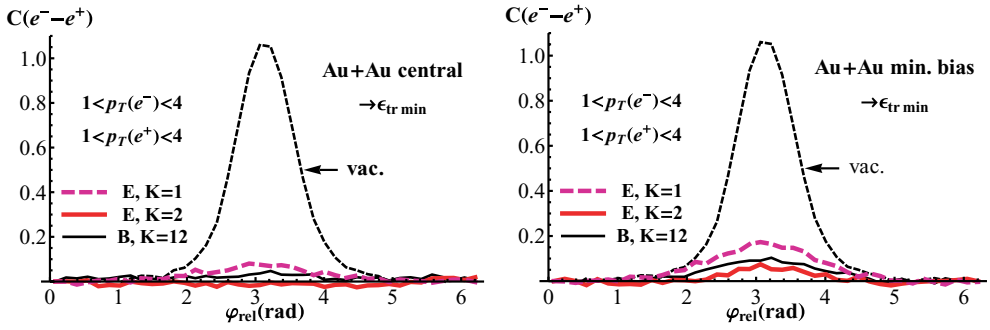

FIG. 14. (Color online) Azimuthal correlation of e^+-e^- nonphotonic pairs as a function of the relative angle for model E and for both, central (left) and minimum bias (right), collisions; Q and $\bar{Q}$ are assumed to be produced back to back and the nonphotonic e^+-e^- background from uncorrelated pairs has been subtracted.

the final state particle. We start from

$$-\frac{dE_\mu}{dx}\Big|_{|t|>|t^*|}^{v\to 1} = \int \frac{d^3k}{(2\pi)^3 2k} n_F(k) \int_{t_{\min}}^{t^*} dt(-t) d_F \frac{d\sigma}{dt}$$
$$= \frac{d^3k}{(2\pi)^3 2k} n_F(k) \int_{t_{\min}}^{t^*} dt(-t) \frac{1}{16\pi(s-M^2)^2}$$
$$\times \frac{1}{d} 32 g^4 \left[\frac{(s-M^2)^2}{t^2} + \frac{s}{t} + \frac{1}{2}\right], \quad \text{(A1)}$$

where M is the mass of the muon, and n_F is the Fermi-Dirac distribution for a massless fermion. As

$$\frac{1}{(s-M^2)^2} \int_{t_{\min}}^{t^*} dt(-t) \left[\frac{(s-M^2)^2}{t^2} + \frac{s}{t} + \frac{1}{2}\right]$$
$$\approx \ln\frac{|t_{\min}|}{|t^*|} - \frac{3}{4} \approx \ln\frac{s}{|t^*|} - \frac{3}{4} \quad \text{(A2)}$$

for $s \gg M^2 \gg |t^*|$, we have

$$-\frac{dE_\mu}{dx}\Big|_{|t|>|t^*|}^{v\to 1} \approx \frac{g^4}{16\pi^4} \int \frac{k}{e^{k/T}+1} \left(\ln\frac{s}{|t^*|} - \frac{3}{4}\right) dk\, d\Omega, \quad \text{(A3)}$$

where $s = M^2 + 2Ek(1-\cos\theta(\vec{p},\vec{k}))$ and where the integral is performed in principle over a domain such that $|t_{\min}| \approx s \geqslant |t^*|$. For $E \gg M \gg |t^*|^{\frac{1}{2}}$, one can nevertheless argue on a physical basis that there is enough "hardness" in almost every collision in order to fulfill this condition, and the domain in which this is not the case becomes negligible. We will therefore integrate over the whole k space as the integral converges. Introducing $u = 1-\cos\theta(\vec{p},\vec{k}) \in [0,2]$, the angular integral leads to

$$\int d\Omega \to 2\pi \int_0^2 \left(\ln\frac{M^2+2Eku}{|t^*|} - \frac{3}{4}\right) du$$
$$= 4\pi\left(\ln\frac{4Ek+M^2}{|t^*|} + \frac{M^2}{4Ek}\ln\frac{4Ek+M^2}{M^2} - 1 - \frac{3}{4}\right). \quad \text{(A4)}$$

Substituting the variable k by $x = k/T$, we obtain the expression

$$-\frac{dE_\mu}{dx}\Big|_{|t|>|t^*|}^{v\to 1} \approx \frac{g^4T^2}{4\pi^3} \int \frac{x}{e^x+1}\left[\ln\frac{4ETx+M^2}{|t^*|} - \frac{7}{4} + \frac{M^2}{4ETx}\ln\left(1+\frac{4ETx}{M^2}\right)\right] dx. \quad \text{(A5)}$$

Because E is assumed to be $\gg M^2/T$ and because the integral is dominated by intermediate values of $x (x \approx 1)$, one can neglect the last term in the integrand and take $M = 0$ in the first term, and one arrives at

$$-\frac{dE_\mu}{dx}\Big|_{|t|>|t^*|}^{v\to 1} \approx \frac{g^4T^2}{4\pi^3} \int \frac{x}{e^x+1}\left(\ln\frac{4ETx}{|t^*|} - \frac{7}{4}\right) dx$$
$$\approx \frac{g^4T^2}{48\pi}\left[\ln\frac{8ET}{|t^*|} - \gamma - \frac{3}{4} - \frac{\zeta'(2)}{\zeta(2)}\right], \quad \text{(A6)}$$

which is Eq. (7) of Ref. [21].

B. Effective IR regulator

The t integration of Eq. (10) yields

$$\mathcal{I} = \frac{1}{(s-M^2)^2} \int_{t_{\min}}^{0} dt(-t) d_F \frac{d\sigma_F}{dt}$$
$$= \frac{1}{(s-M^2)^2} \int_0^{|t_{\min}|} \Big(-\mu^2 * \frac{(s-M^2)^2}{(|t|+\mu^2)^2} + \frac{(s-M^2)^2+\mu^2 s}{|t|+\mu^2} - s + \frac{|t|}{2}\Big) d|t|$$
$$= \left(1+\frac{\mu^2 s}{(s-M^2)^2}\right)\ln\left(1+\frac{(s-M^2)^2}{\mu^2 s}\right) - 1 + \frac{(s-M^2)^2}{4s^2} - \underbrace{\frac{|t_{\min}|}{|t_{\min}|+\mu^2}}_{\approx 1}, \quad \text{(A7)}$$

and we obtain for the energy loss

$$-\frac{dE_\mu}{dx}\Big|_{\text{eff}}^{v\to 1} \approx \frac{g^4T^2}{8\pi^3} \int_0^{+\infty} \int_0^2 \frac{x}{e^x+1} \mathcal{I}(s)\, dk\, du, \quad \text{(A8)}$$

where $s = M^2 + 2ETxu$. We first notice that $\frac{\ln(1+a)}{a}$ in $\mathcal{I}$ [with $a = \frac{(s-M^2)^2}{\mu^2 s}$] is maximal and bounded at $a = 0 (s = M^2)$ and then decreases like $\mu^2/s \propto \mu^2/ET$ for larger values of s. It then brings a contribution $\propto \mu^2/ET$ that is subdominant at large energies. In this regime, s is $\gg M^2$ for most of the (u, x) integration domain, so that the third term of $\mathcal{I}$ can be replaced by its asymptotic $1/4$ value, and $|t_{\min}|$ in the logarithm can be replaced by s. Therefore,

$$\mathcal{I} \approx \ln\frac{s+\mu^2}{\mu^2} - \frac{3}{4} - 1 \approx \ln\frac{s+\mu^2}{e\mu^2} - \frac{3}{4}, \quad \text{(A9)}$$

and one realizes that $-\frac{dE_\mu}{dx}|_{\text{eff}}^{v\to 1}$ is nothing but the hard contribution in Eq. (A3) with $|t^*| \to e\mu^2$ and $M^2 \to M^2 + \mu^2 \approx M^2$. We thus can read off the result directly from Eq. (8):

$$-\frac{dE_\mu}{dx}\Big|_{\text{eff}}^{v\to 1} \approx \frac{g^4T^2}{48\pi}\left[\ln\frac{8ET}{e\mu^2} - \gamma - \frac{3}{4} - \frac{\zeta'(2)}{\zeta(2)}\right], \quad \text{(A10)}$$

and obtain Eq. (11).

[1] B. I. Abelev *et al.* (STAR Collaboration), Phys. Rev. Lett. **98**, 192301 (2007).

[2] A. Adare *et al.* (PHENIX Collaboration), Phys. Rev. Lett. **98**, 172301 (2007).

[3] M. Cacciari, P. Nason, and R. Vogt, Phys. Rev. Lett. **95**, 122001 (2005).

[4] G. Martinez-Garcia, S. Gadrat, and P. Crochet, Phys. Lett. **B663**, 55 (2008).

[5] G. D. Moore and D. Teaney, Phys. Rev. C **71**, 064904 (2005).
[6] H. van Hees and R. Rapp, Phys. Rev. C **71**, 034907 (2005).
[7] H. van Hees, V. Greco, and R. Rapp, Phys. Rev. C **73**, 034913 (2006).
[8] V. Greco, H. van Hees, and R. Rapp, arXiv:0709.4452 [hep-ph].
[9] P. B. Gossiaux, V. Guiho, and J. Aichelin, J. Phys. G **31**, S1079 (2005).
[10] P. B. Gossiaux, V. Guiho, and J. Aichelin, J. Phys. G **32**, S359 (2006).
[11] D. Molnar, J. Phys. G **31**, S421 (2005).
[12] B. Svetitsky, Phys. Rev. D **37**, 2484 (1988).
[13] Ben-Wei Zhang, Enke Wang, and Xin-Nian Wang, Phys. Rev. Lett. **93**, 072301 (2004).
[14] N. Armesto, M. Cacciari, A. Dainese, C. A. Salgado, and U. A. Wiedemann, Phys. Lett. **B637**, 362 (2006).
[15] B. L. Combridge, Nucl. Phys. **B151**, 429 (1979).
[16] P. Chakraborty, M. G. Mustafa, and M. H. Thoma, Phys. Rev. C **75**, 064908 (2007).
[17] M. G. Mustafa, Phys. Rev. C **72**, 014905 (2005); Acta. Phys. Hung. A Heavy Ion Phys. **22**, 93 (2005).
[18] M. Djordjevic and M. Gyulassy, Nucl. Phys. **A733**, 265 (2004).
[19] B. G. Zakharov, JETP Lett. **86**, 444 (2007).
[20] H. A. Weldon, Phys. Rev. D **26**, 1394 (1982).
[21] E. Braaten and M. H. Thoma, Phys. Rev. D **44**, 1298 (1991); **44**, R2625 (1991).
[22] S. Peigné and A. Peshier, Phys. Rev. D **77**, 014015 (2008).
[23] S. Peigné and A. Peshier, Phys. Rev. D **77**, 114017 (2008).
[24] Y. L. Dokshitzer, G. Marchesini, and B. R. Webber, Nucl. Phys. **B469**, 93 (1996).
[25] A. C. Mattingly and P. M. Stevenson, Phys. Rev. D **49**, 437 (1994).
[26] S. J. Brodsky, S. Menke, C. Merino, and J. Rathsman, Phys. Rev. D **67**, 055008 (2003).
[27] A. Peshier, arXiv:hep-ph/0601119; Phys. Rev. Lett. **97**, 212301 (2006).
[28] S. Wicks and M. Gyulassy, J. Phys. G **34**, S989 (2007).
[29] D. B. Walton and J. Rafelski, Phys. Rev. Lett. **84**, 31 (2000).
[30] Jen-Chieh Peng and Mike Leitch (private communication).
[31] P. Kolb and U. Heinz, in *Quark Gluon Plasma,* edited by R. Hwa and X. N. Wang (World Scientific, Singapore, 2002).
[32] W. A. Horowitz and M. Gyulassy, presented at the 20th International Conference on Ultra-Relativistic Nucleus-Nucleus Collisions: Quark Matter 2008 (QM2008), Jaipur, India, 4–10 Feb. 2008 (unpublished), arXiv:0804.4330 [hep-ph].